

Recycling of spent magnesite and ZAS bricks for the production of new basic refractories

A.G.M. Othman^{*}, W.M.N. Nour

Department of Refractories, Ceramics, and Building Materials, National Research Centre, 12622 Dokki, Cairo, Egypt

Received 17 September 2003; received in revised form 16 September 2004; accepted 7 November 2004

Available online 16 February 2005

Abstract

Changing environmental awareness and regulations, the cost of waste disposal, and concerns about future liabilities have caused increased interest in recycling of spent refractories. The densification parameters of spent magnesite containing up to 10.0 wt.% spent ZAS (zirconium aluminium silicate) sintered at 1450–1550 °C were investigated. X-ray, microstructure and microchemistry analysis were used to establish the present phases. The technological parameters in terms of RUL (refractoriness under load) and TSR (thermal shock resistance) of the prepared refractories attaining their maximum densification were evaluated. The results revealed that, the addition of spent ZAS up to 5.0 wt.% to spent magnesite enhanced the physico-mechanical, refractory and thermal properties due to the development of highly refractory phases MA spinel and MgO·ZrO₂ solid solution. Samples containing more than 5.0 wt.% spent ZAS exhibited lower refractory and thermal properties due to the formation of M₂S ferroan beside the high flux CMS phase.

© 2005 Elsevier Ltd and Techna Group S.r.l. All rights reserved.

Keywords: Recycling; Magnesite; ZAS

1. Introduction

The recovery and recycling of refractories is now of even greater importance than ever. Refractories recycling is an important issue from the standpoint of waste minimization. Waste management is a very important issue from the public health perspective, the environmental and industrial view points, because an ever-increasing amount of hazardous materials need to be disposed in a safe and economical way or, preferably, reused whenever possible. In fact, the waste produced by a given industry can often be regarded as useful raw materials to be recycled, thus reducing the negative environmental impact associated with landfill, cost saving and preserving non-renewable natural resources.

The recycling of waste refractories into raw materials for the production of new refractories is normally the area where the value is the highest. The demands on purity and compositional consistency of the raw materials make characterization of the spent refractories important. In general,

the level of contamination is high for used monolithics in comparison with shaped refractories. Spent refractories can be utilized in a number of applications, including: new refractories; slag conditioner; cement component; concrete aggregate; road aggregate; and glass raw material [1–3].

The recycling rate for by products of metallurgical production will be enhanced in the future. The steel and glass industries are highly concerned with a considerable amounts of magnesite and zirconium aluminosilicate (ZAS) waste bricks, respectively, that are produced annually and the problems related with waste management, storage and/or transportation costs for disposal.

According to the strongly basic nature and high fusion temperature of magnesia (2800 °C), it can be used as a refractory in contact with basic slags and other basic fluxes. It is used to produce ceramically-bonded bricks with numerous applications particularly in ferrous industries because of its high resistance to attack by FeO- and Fe₂O₃-rich slags and also as a lining for the high temperature zone of rotary cement kiln as well as in rotary lime kiln. Magnesia can be derived from naturally magnesite rock (MgCO₃) which contains some fluxing oxides as Fe₂O₃, SiO₂, Al₂O₃

^{*} Corresponding author. Fax: +20 0233 70931.

E-mail address: agmothman@yahoo.com (A.G.M. Othman).

and CaO or synthetically as sea-water magnesium hydroxide ($\text{Mg}(\text{OH})_2$) with low B_2O_3 content [4–6]. The technological changes in the iron and steel as well as other metallurgical industries need development of magnesite refractories. These development involves the use of new magnesia bricks in the form of MgO –C [7–9] as well as Al_2O_3 [10], TiO_2 [11,12] and ZrO_2 [13] to increase its mechanical properties, wear and corrosion. Such improvement requires the use of high purity MgO with low B_2O_3 and other fluxing oxides as well as increasing the CaO/SiO_2 molar ratio up to 2.0 which leads to form direct bonded magnesia grains with higher refractory quality and low liquid phase content.

The largest part of the spent refractories in iron and steel industry is dolomite, followed by magnesite, then fireclay and bauxite. About 95.0% of the excavated refractory materials are recycled [14].

ZAS is one of the most famous lining bricks for glass industries. It consists mainly of corundum, mullite and zirconia. Brick grades with a ZrO_2 content ranged between 31 and 42% are manufactured by fusion casting. These bricks are distinguished by high corrosion resistance against several types of aggressive media. The corrosion resistance increases with growing ZrO_2 content. During cooling of the brick melt, baddeleyite (monoclinic ZrO_2), and corundum are precipitated and interpenetrated at the same time. In the glassy solidified residual melt (approximately 20%) there are round ZrO_2 crystals, which protect the less resistance corundum from attack by the glass melt [15].

The aim of this work is to investigate the preparation of a good quality magnesite refractories from spent magnesite bricks as a raw material with different spent ZAS proportions (up to 10.0 wt.%). The physical, mineralogical composition, microstructure, mechanical, thermal and refractory properties of the prepared bodies are studied.

2. Experimental procedure

Characterization of the spent materials to identify impurities and their quantity is important to find a suitable use. The starting materials are magnesite and ZAS waste bricks from rotary kiln of lime and glass industries, respectively. The elemental composition of the starting materials was performed by XRF (PW 1400 Philips) and presented in Table 1. The results indicated that MgO is the major constituent (~ 94 wt.%) besides SiO_2 , Al_2O_3 , CaO and Fe_2O_3 as a minor constituents in the used magnesite. The CaO/SiO_2 molar ratio is 1.276. The main constituents of the used ZAS are Al_2O_3 , ZrO_2 and SiO_2 .

Phase analysis of the starting materials were performed using X-ray diffractometry (XRD; Model PW/1710) using $\text{Cu K}\alpha$ radiation and operated at 50 kV and 300 mA. Fig. 1a and b shows that periclase is the major phase besides monticellite (CMS) as the minor phase in the magnesite waste, whereas corundum, baddeleyite, cristobalite and zircon are the detected phases in the used ZAS.

Table 1

Chemical composition of the used wastes (mass%)

Oxides	Used magnesite bricks	Used ZAS bricks
SiO_2	1.51	17.62
Al_2O_3	0.62	46.11
Fe_2O_3	1.55	0.01
TiO_2	–	0.20
ZrO_2	–	31.19
Na_2O	–	3.10
K_2O	–	0.10
CaO	1.80	1.60
MgO	93.84	0.02
Others	–	0.05
LOI	0.68	–

Eight batches were made by thoroughly mixing magnesite and ZAS powders (0.1 mm) in a ball mill jar for 2 h. The percentages of ZAS in the batches as shown in Table 2 were 0, 1, 2, 3, 4, 5, 7 and 10 wt.%, which symbolized by M_0 , M_1 , M_2 , M_3 , M_4 , M_5 , M_7 and M_{10} , respectively.

Approximately 25 g of the milled powder mixture was uniaxially pressed to 2.5 cm diameter compacts at a pressure of 1 t/cm^2 and 5 wt.% glycerin was added as a binder during pressing. The green compacts were dried at 110°C for 24 h then densified at 1450 – 1550°C for 2 h.

Densities and porosities were determined by Archimedes immersion technique using kerosine. The permanent linear change was determined. The cold crushing strength of the fired compacts was measured using a compressive strength

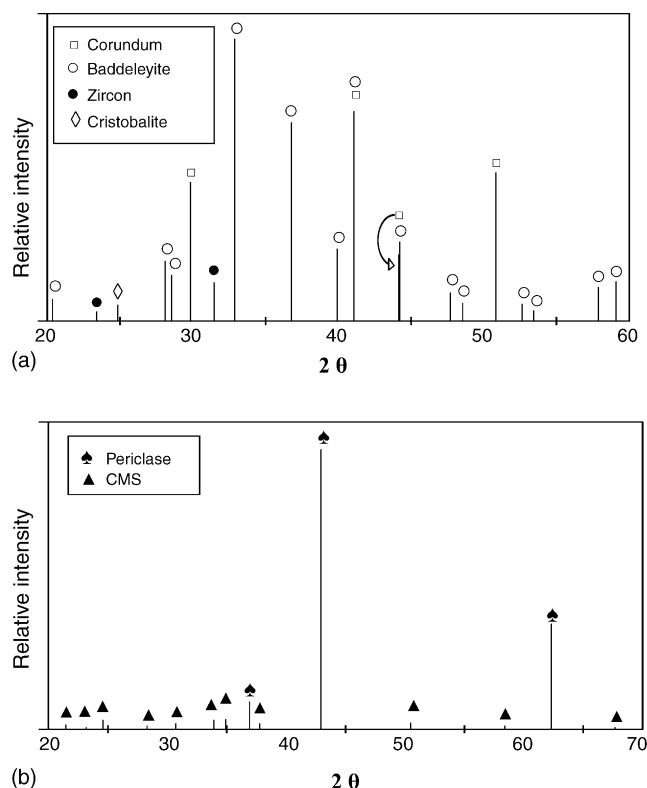


Fig. 1. XRD patterns of (a) used magnesite waste and (b) used ZAS waste.

Table 2
Batch design and chemical compositions of the investigated samples

Sample number	Batch composition (wt.%)		Chemical composition (wt.%)								
	Used magnesite	Used ZAS	MgO	Al ₂ O ₃	SiO ₂	ZrO ₂	CaO	Fe ₂ O ₃	Na ₂ O	Others	CaO/SiO ₂ molar ratio
M ₀	100	–	94.48	0.62	1.52	–	1.81	1.56	–	–	1.272
M ₁	99	1	93.53	1.07	1.68	0.31	1.81	1.54	0.03	0.01	1.152
M ₂	98	2	92.59	1.53	1.84	0.62	1.80	1.53	0.06	0.01	1.050
M ₃	97	3	91.65	1.98	2.00	0.93	1.80	1.51	0.09	0.01	0.965
M ₄	96	4	90.78	2.44	2.16	1.25	1.80	1.50	0.12	0.01	0.892
M ₅	95	5	89.76	2.89	2.32	1.56	1.80	1.48	0.16	0.02	0.829
M ₇	93	7	87.87	3.80	2.65	2.18	1.79	1.45	0.22	0.02	0.726
M ₁₀	90	10	85.03	5.17	3.13	3.12	1.79	1.40	0.31	0.02	0.612

machine of the SEIDNER; Riedlinger type, Germany, having a maximum load capacity of 600 kN.

The microstructure of some selected fired compositions at 1550 °C was examined using scanning electron micro-

scope (SEM; Model Philips XL30) attached with an energy dispersive X-ray analysis (EDAX).

The refractory quality of the compacts sintered at 1550 °C was tested using refractoriness under-load test up

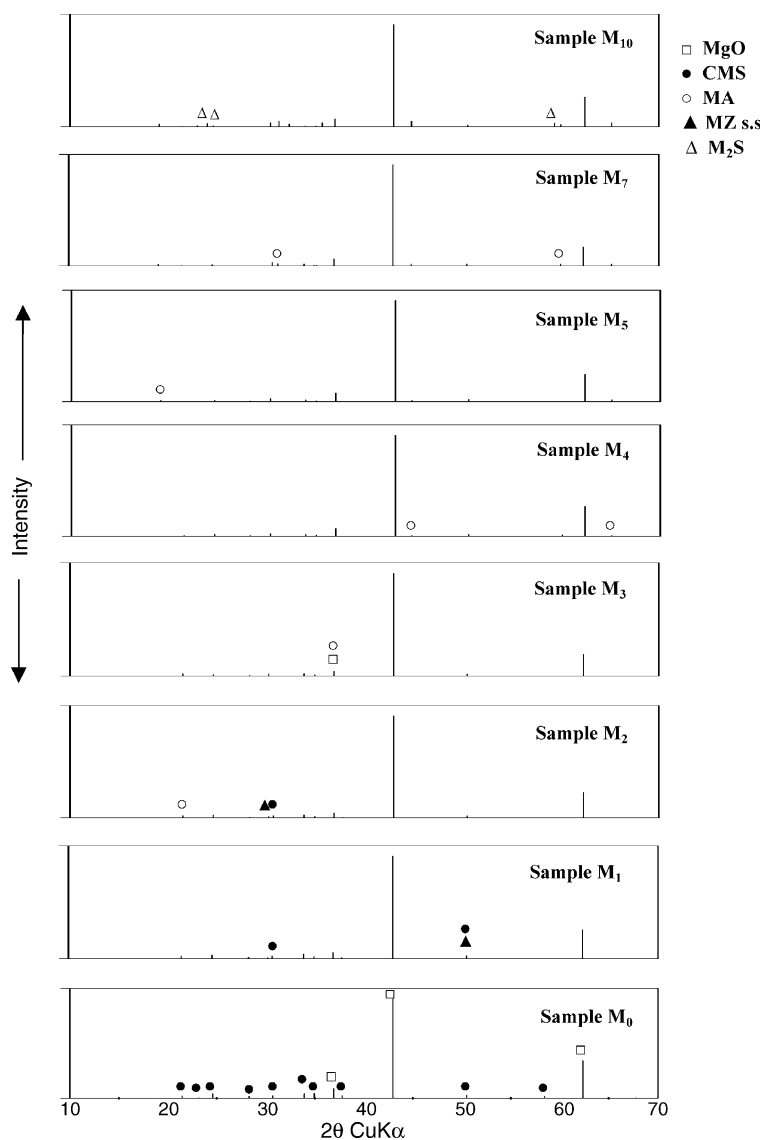


Fig. 2. XRD patterns of the investigated samples sintered at 1550 °C/2 h.

to 1500 °C (DIN 51064). Thermal shock experiments were performed by introducing the sintered compacts into a muffle furnace maintained at 1000 °C and then quenched in air after 15 min. Thermal cycling was performed by reheating the compacts to the same temperature and quenching up to 30 times. Compacts properties were measured after 30 thermal shock cycles to assess the extent of damage.

3. Results and discussion

3.1. Phase evolution and densification parameters

XRD patterns of the investigated samples sintered at 1550 °C for 2 h are shown in Fig. 2. It can be seen that periclase is the major phase besides CMS phase in sample M_0 . The CaO/SiO₂ molar ratio in these compositions ranged between 1.276 for M_0 and 0.612 for M_{10} (Table 2). Accordingly, the lines intensity of CMS was decreased with decreasing CaO/SiO₂ molar ratio with the appearance of forsterite (M_2S ferroan) at the expense of CMS (monticellite) in M_{10} sample. Moreover, on increasing ZAS content, the amounts of Al₂O₃ and ZrO₂ increase leading to the appearance of new lines of MA as well as the lines intensity of magnesia zirconia (s.s) increased. Nandi et al. [16] concluded that in MgO-based compositions, the presence of SiO₂ enhances spinel formation. Also, it was found that increasing SiO₂ decreases the spinel content when fired at lower temperatures (\approx 1450 °C). At higher temperatures, it was concluded that spinel formation increases. SiO₂ favours spinel formation through dissolution and recrystallization. MA spinel possesses an unusual combination of

properties and is an important phase in ceramic science. High melting point, excellent high temperature mechanical, thermal, chemical and spalling properties lead to an essential refractory item for many applications, namely, lining materials [17].

Microstructure is as important as bulk composition in determining the physico-mechanical properties of refractories. SEM micrographs of samples M_0 , M_1 and M_5 are shown in (Fig. 3). Fig. 3A revealed a relatively large grains of periclase. A predominance of direct contacts was observed. EDAX pattern of the considered phase was shown in Fig. 4a. Around the periclase grain boundaries some ferrites are shown as magnesioferrites (light white). In addition, relatively high pore content with different pore size were observed. On the other hand, addition of 1.0 wt.% ZAS to magnesite (sample M_1) leads to the appearance of a rounded and subrounded grains of periclase phase surrounded by some magnesium silicates and ferrites in solid solution as appeared in (Fig. 3B) and detected in (Fig. 4b). Also, white needles-like shape of spinel structure beneath the periclase grains was clearly seen by close examination of their microstructure as shown in (Fig. 3C). MgO:Al₂O₃ ratio of needles, determined by EDAX, was \sim 1:1.5 (Fig. 4c). On further addition of ZAS (5.0 wt.%, sample M_5) as shown in (Fig. 3D), some magnesia zirconia (s.s), magnesium silicate phases as CMS and M_2S ferroan and magnesium ferrite precipitated inside some pores. The Point analysis of these phases are observed in (Fig. 4d). As well as, white needles-like shape of spinel structure was growth in their size and increased in amount forming a cluster in beneath of periclase grains. These needles were detected as shown in (Fig. 4e). These results are confirmed with the X-ray analysis data as shown in (Fig. 2).

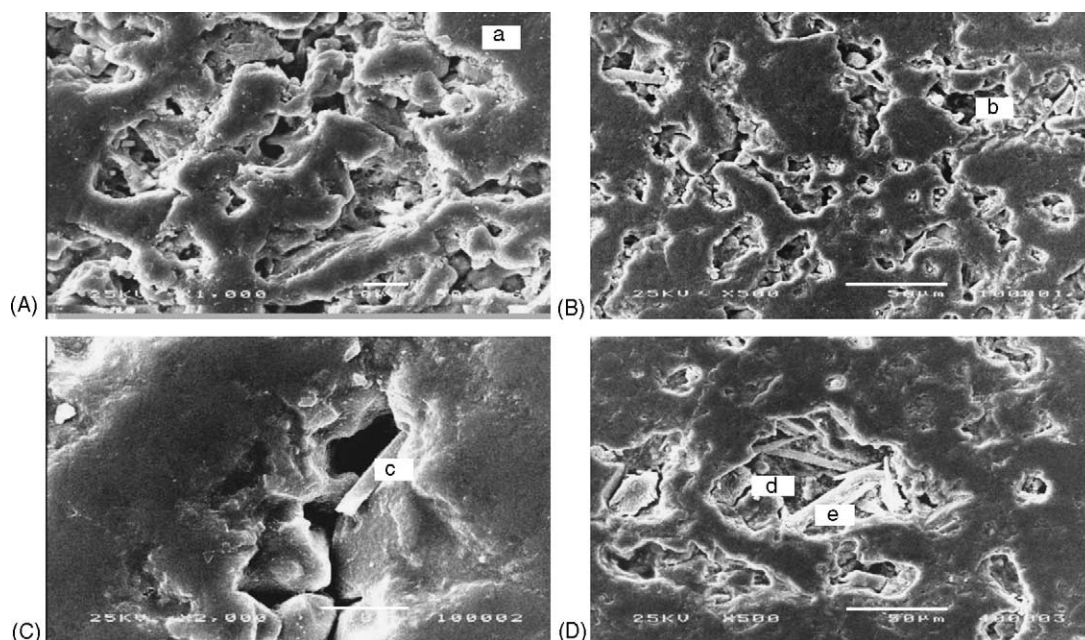


Fig. 3. SEM micrographs of samples M_0 , M_1 and M_5 sintered at 1550 °C.

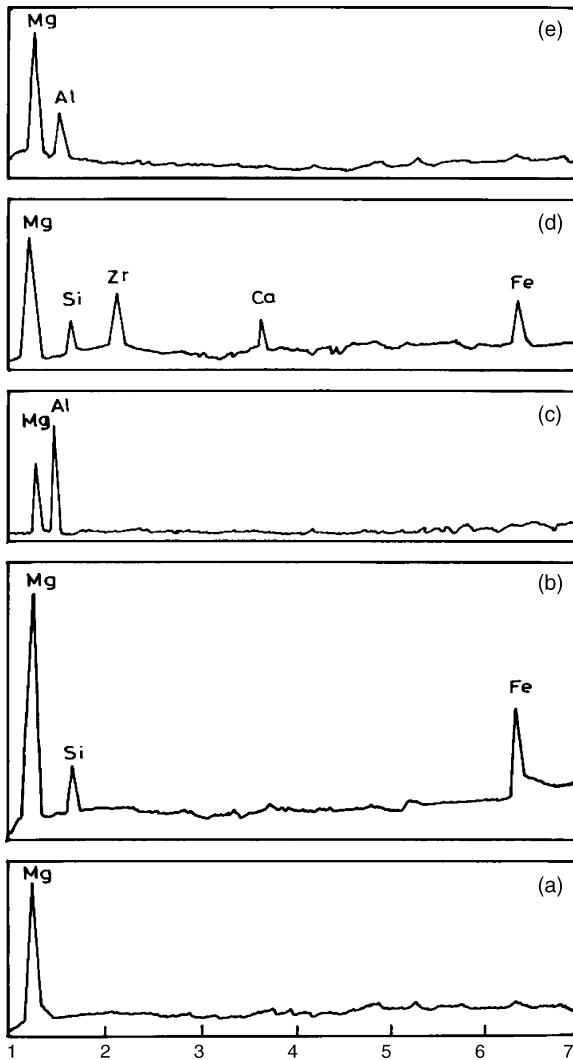


Fig. 4. EDAX patterns of: sample M_0 , Point (a); sample M_1 , Point (b) and (c); samples M_5 , Point (d) and (e).

Figs. 5–7 exhibit the densification parameters of the investigated samples in terms of bulk density, apparent porosity and linear shrinkage, respectively, as a function of firing temperature up to 1550 °C and ZAS wt.% additions. It

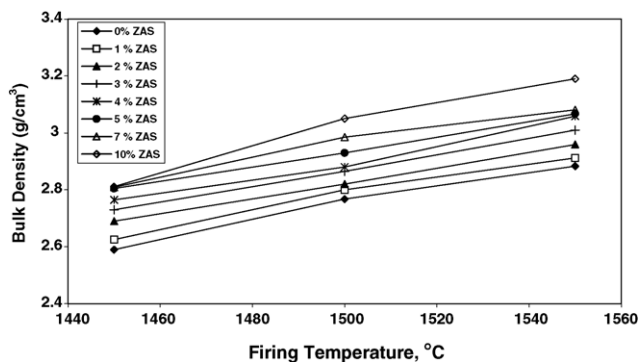


Fig. 5. Effect of firing temperature on the bulk density of the investigated samples.

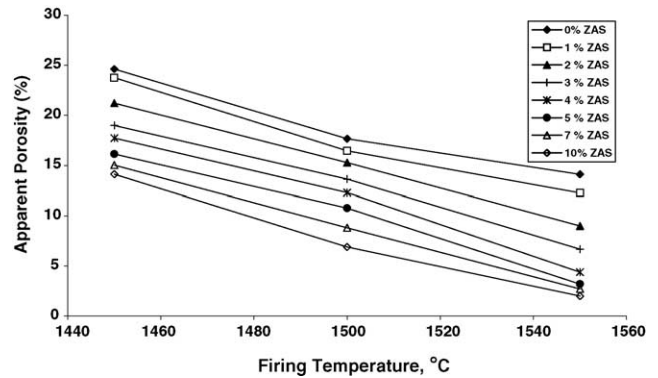


Fig. 6. Effect of firing temperature on the apparent porosity of the investigated samples.

is evident that as the firing temperature and the amount of ZAS was increased, the samples densified as indicated by the increase in both of the bulk density and linear shrinkage with simultaneous decrease in apparent porosity which reaches its maximum value at 1550 °C and 10.0 wt.% ZAS. Such densification was attributed to the formation of liquid phases within the samples, i.e. vitrification takes place in a steady state. CMS and M_2S are the distinct phases responsible for increasing the amount of liquid phase in the prepared briquettes. These phases crystallize on cooling around MgO and MA and also in pores resulting in enhancement of the densification parameters. The increase in bulk density of these samples upon ZAS additions is also attributed to the partial replacement of magnesite of lower density by ZAS of higher density. The associated volume expansion, theoretically 5–7%, accompanying the formation of spinel—from the reaction of Al_2O_3 with MgO—partially offsets the subsequent shrinkage due to liquid phase formation. This interpreted the results of linear shrinkage of samples containing more than 5.0 wt.% ZAS which exhibit lower linear shrinkage.

The higher bulk density of the samples fired up to 1550 °C resulted in high cold crushing strength values, especially, in the presence of higher concentrations of ZAS (up to 5.0 wt.%) (Fig. 8). However, samples containing more than 5.0 wt.% ZAS showed lower values of CCS. Such

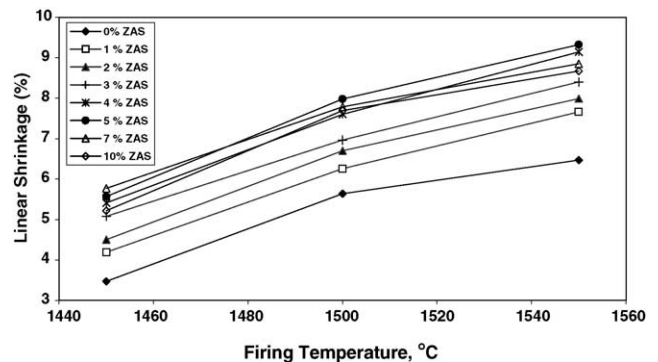


Fig. 7. Effect of firing temperature on the linear shrinkage of the investigated samples.

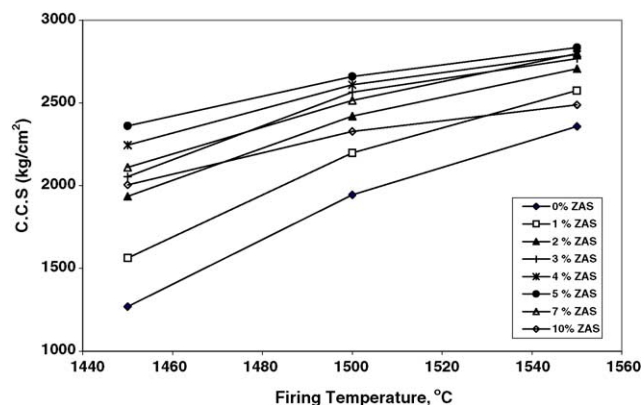


Fig. 8. Effect of firing temperature on cold crushing strength of the investigated samples.

decrease may be attributed to microcrack formation due to the difference between thermal expansion coefficient of spinel, $\text{MgO} \cdot \text{ZrO}_2 \cdot \text{s}$ and periclase. In a similar work, Nourbakhsh et al. [18] indicated that higher amounts of spinel (10.0 wt.%) resulted in intense decrease in CCS (cold crushing strength) of MgO refractories. In general, the cold crushing strength values increase with firing temperature from 1450 to 1550 °C. This indicates that the more developed glassy phases at higher temperatures providing the crystalline phases with a strong bond.

3.2. Technical properties

3.2.1. Refractoriness under-load

Samples attaining their maximum densification quality at 1550 °C were tested for their flow behaviour under-load and the results are summarized in Table 3. The results indicate that testing of lower sinterability samples results in an earlier subsidence behaviour due to their volume unstability. At the same time, the gradual improvement in the refractory quality of samples containing ZAS up to 5.0 wt.% may be attributed to the more development of highly refractory MA and $\text{MgO} \cdot \text{ZrO}_2 \cdot \text{s}$ phases as confirmed by X-ray analysis (Fig. 2) in addition to the high refractory property of periclase. On the other hand, excessive liquid phases of M_2S ferroan of low refractory property as well as the presence of relatively high fluxing oxides in samples containing more than

Table 3

Refractoriness under-load of the tested samples fired at 1550 °C

Sample number	AP (%)	Beginning of subsidence (°C)	$T_{0.6}$ (°C)
M ₀	14.10	1450	1490
M ₁	12.25	1450	1490
M ₂	8.99	1465	>1500
M ₃	6.67	1480	>1500
M ₄	4.37	1495	>1500
M ₅	3.18	>1500	>1500
M ₇	2.71	1470	>1500
M ₁₀	1.99	1425	1470

5.0 wt.% ZAS (samples M₇ and M₁₀) retard the positive effect of the highly refractory phases in improving the refractory quality of these samples. Sample M₁₀ shows the lowest temperature at 0.6% sagging occurred (Table 3).

3.2.2. Thermal shock resistivity

The aim of thermal shock testing is to provide information on the ability of a refractory body to undergo one or many rapid changes in temperature without damage. This characterization can be qualitative (chiefly by visual inspection) or quantitative (by measuring the variation of a given property of the body). The results of thermal shock testing of all tested samples indicated that heating the samples up to 1000 °C then quenching in air for 30 thermal cycles did not cause any visually observed damage. The effect of thermal shock cycling up to 30 cycles on the densification parameters of the tested samples was shown in Table 4. It is generally agreed that an expected reduction in densification parameters of refractories subjected to thermal cycling. This is the case in our results, which can be attributed to the generation of mechanical stress therein. On exceeding the mechanical strength threshold, elastic strain energy is released, which accompanied by the formation and propagation of microcracks. The thermal mismatch between the different phases in the tested refractory bodies are also responsible for generating microcracks. Samples M₇ and M₁₀ were the most degraded ones, whereas sample M₀ showed the lowest degradation. The role of porosity in enhancing the resistance to thermal shock damage is well known where pores helps to arrest excessive crack

Table 4

Densification parameters of the tested samples fired at 1550 °C before and after 30 thermal shock cycles

Sample number	Before thermal cycling			After thermal cycling			Percent change		
	BD (g/cm ³)	AP (%)	CCS (kg/cm ²)	BD (g/cm ³)	AP (%)	CCS (kg/cm ²)	BD	AP	CCS
M ₀	2.88	14.10	2358	2.86	13.72	2275	−0.69	2.69	−3.52
M ₁	2.91	12.25	2575	2.88	11.85	2471	−1.03	3.26	−4.04
M ₂	2.96	8.99	2707	2.93	8.63	2581	−1.01	4.00	−4.65
M ₃	3.01	6.67	2768	2.97	6.38	2609	−1.32	4.35	−5.74
M ₄	3.06	4.37	2793	3.02	4.55	2652	−1.31	4.12	−5.05
M ₅	3.07	3.18	2835	3.04	3.30	2700	−0.98	3.77	−4.76
M ₇	3.08	2.71	2798	3.02	2.87	2523	−1.95	5.90	−9.83
M ₁₀	3.19	1.99	2489	3.07	2.23	2104	−3.76	12.06	−15.47

propagation. On the other hand, repeated heating and cooling impaired the properties of the glassy phases binding the crystalline phases as a result of their high temperature coefficient of linear expansion. The relatively good thermal shock resistivity of samples M_4 and M_5 may be attributed to their moderate porosity, in addition to the presence of MA and $MgO\text{-}ZrO_2$ s.s. It is found [18–20] that $MgO\text{-}ZrO_2$ composites have better performance on thermal shock resistance than magnesite-based materials. Crack formation around the spinel aggregates is a mechanism for increasing thermal shock resistance of MgO -spinel refractories [20].

4. Conclusions

- (1) The addition of derived spent ZAS used as lining for glass kiln up to 5.0 wt.% to spent magnesite obtained from rotary lime kiln enhances the densification, refractory and thermal parameters due to the formation of highly refractory phases (MA and $MgO\text{-}ZrO_2$ s.s).
- (2) Excessive liquid phase of M_2S ferroan of low refractory properties as well as the presence of relatively high fluxing oxides in samples containing more than 5.0 wt.% ZAS retard the positive effect of the highly refractory phases in improving the refractoriness under-load and thermal shock resistivity.

References

- [1] A. O. Valoref, Recovery and recycling of scrap refractories, *World Ceram. Refract.* 9 (1998) 13–16.
- [2] Y. Nakamura, N. Hirai, Y. Tsutsui, K. Uchinokura, S.I. Tamura, Recycling of refractories in the steel industry, *Ind. Ceram.* 19 (2) (1999) 111–114.
- [3] C. Viklund-White, K. Ruotanen, S. Gehör, Spent ladle refractories-characterisation and reuse in new refractory materials, in: *International Colloquium on Refractories*, Aachen, Germany, 2001, pp. 86–91.
- [4] J.H. Chester, *Refractories, Production and Properties*, Iron and Steel Institute, London, 1973.
- [5] D.R.F. Spencer, Basic refractory raw materials, *Trans. J. Br. Ceram. Soc.* 71 (1972) 123–134.
- [6] J. White, in: A.M. Alper (Ed.), *High Temperature Oxides*, vol. 7, Academic Press, New York, 1970.
- [7] D.T. Evans, J. Quin, P.G. Whiteley, Magnesia-graphite refractories for basic oxygen converters, *Steel Techn. Int.* (1994) 105–108.
- [8] A. Yamaguchi, Progress of the carbon containing refractories in recent years, *Inorg. Mater.* 4 (1997) 85–91.
- [9] P. Jeschke, G. Mortel, Recent tendencies in refractories for iron and steel production, in: *UNITCER 93 Proceedings*, Sao Paulo, 1993, pp. 1–15.
- [10] I. Teoreanu, N. Ciocea, Magnesia-alumina spinel for refractories, *Interceram* 36 (1987) 19–21.
- [11] M. Nath Chaudhuri, A. Kumar, A.K. Bhardra, G. Banerjee, Sintering and grain growth in Indian magnesites doped with titanium dioxide, *Interceram* 39 (1990) 26–30.
- [12] M. Nath Chaudhuri, A. Kumar, A.K. Bhardra, G. Banerjee, Microstructure of sintered natural Indian magnesites with titania addition, *Ceram. Bull.* 71 (1992) 345–348.
- [13] Z.M. Naziri, Einsatz von thermisch hochbelastbaren magnesia-zirkonsteinen in schacht und drehrohröfen, *Zement-kalk-Gips* 48 (1995) 224–230.
- [14] N. Bannenberg, K.J. Arlt, Utilisation of used refractory material and slag as secondary raw materials, *Veitsch-Radex-Rundschau* 1 (1997) 3–10.
- [15] G. Roulschka, *Pocket Manual Refractory Materials*, Vulkan-Verlag, Essen, 1997, pp. 115–123.
- [16] P. Nandi, A. Grag, B.D. Chattoraj, M.S. Mukhopadhyay, Effect of silica and temperature on spinel based high-alumina castables, *Am. Ceram. Soc. Bull.* 79 (12) (2000) 65–69.
- [17] R.D. Maschio, B. Fabbri, C. Fiori, Industrial applications of refractories containing magnesium aluminate spinel, *Ind. Ceram.* 8 (1988) 121–126.
- [18] A.A. Nourbakhsh, B. Doroushi, S.M. Hejazi, S. Otroj, Development of MgO refractories by using synthesized spinel for application in steel industries, in: *Proceedings of the 44th International Colloquium on Refractories*, Aachen, September 2001, pp.104–107.
- [19] R.E. Carter, Mechanism of solid state reaction between $MgO\text{-}Al_2O_3$ and $MgO\text{-}Fe_2O_3$, *J. Am. Ceram. Soc.* 44 (1965) 116–120.
- [20] B. Zhu, N. Li, F. Gan, R. Chen, S. Tian, Effects of composition of fused magnesia-zirconia material on its microstructure and properties, *Refractories* 34 (2000) 130–132.